Tumor-associated neutrophils stimulate T cell responses in early-stage human lung cancer

Evgeniy B. Eruslanov,[1] Pratik S. Bhojnagarwala,[1] Jon G. Quatromoni,[1] Tom Li Stephen,[2] Anjana Ranganathan,[3] Charuhas Deshpande,[4] Tatiana Akimova,[5] Anil Vachani,[6] Leslie Litzky,[4] Wayne W. Hancock,[5] José R. Conejo-Garcia,[2] Michael Feldman,[4] Steven M. Albelda,[6] and Sunil Singhal[1]

[1]Division of Thoracic Surgery, Department of Surgery, Perelman School of Medicine at the University of Pennsylvania, Philadelphia, Pennsylvania, USA. [2]Tumor Microenvironment and Metastasis Program, The Wistar Institute, Philadelphia, Pennsylvania, USA. [3]Division of Hematology/Oncology and [4]Department of Pathology and Laboratory Medicine, Perelman School of Medicine at the University of Pennsylvania, Philadelphia, Pennsylvania, USA. [5]Division of Transplant Immunology, Department of Pathology and Laboratory Medicine, Children's Hospital of Philadelphia and Perelman School of Medicine at the University of Pennsylvania, Abramson Research Center, Philadelphia, Pennsylvania, USA. [6]Division of Pulmonary, Allergy, and Critical Care, Department of Medicine, Perelman School of Medicine at the University of Pennsylvania, Philadelphia, Pennsylvania, USA.

Infiltrating inflammatory cells are highly prevalent within the tumor microenvironment and mediate many processes associated with tumor progression; however, the contribution of specific populations remains unclear. For example, the nature and function of tumor-associated neutrophils (TANs) in the cancer microenvironment is largely unknown. The goal of this study was to provide a phenotypic and functional characterization of TANs in surgically resected lung cancer patients. We found that TANs constituted 5%–25% of cells isolated from the digested human lung tumors. Compared with blood neutrophils, TANs displayed an activated phenotype (CD62L^{lo}CD54^{hi}) with a distinct repertoire of chemokine receptors that included CCR5, CCR7, CXCR3, and CXCR4. TANs produced substantial quantities of the proinflammatory factors MCP-1, IL-8, MIP-1α, and IL-6, as well as the antiinflammatory IL-1R antagonist. Functionally, both TANs and neutrophils isolated from distant nonmalignant lung tissue were able to stimulate T cell proliferation and IFN-γ release. Cross-talk between TANs and activated T cells led to substantial upregulation of CD54, CD86, OX40L, and 4-1BBL costimulatory molecules on the neutrophil surface, which bolstered T cell proliferation in a positive-feedback loop. Together our results demonstrate that in the earliest stages of lung cancer, TANs are not immunosuppressive, but rather stimulate T cell responses.

Introduction

Murine and human studies suggest that tumor initiation and progression are commonly accompanied by "smoldering" inflammation (1). Tumor-infiltrating myeloid cells represent a significant proportion of the inflammatory cell population in the tumor microenvironment, and they influence nearly every step in tumor progression, including the suppression of adaptive immunity, the promotion of neoangiogenesis and lymphangiogenesis, the remodeling of the extracellular matrix, the promotion of invasion and metastasis, and lastly, the inhibition of vaccine-induced antitumor T cell responses (2). Among the different types of myeloid cells, tumor-associated macrophages (TAMs) have been the best characterized and are generally considered protumoral in murine tumor models (3, 4). The role of tumor-associated neutrophils (TANs) in cancer progression remains unclear and has been investigated only recently in murine models. Characterization of human TANs is even less well developed.

In murine studies, TANs appear to have dichotomous protumor and antitumor effects (5–7). Similar to the classic (M1) and alternative (M2) activation pathways proposed for TAMs, the paradigm of antitumor "N1 neutrophils" versus protumoral "N2

neutrophils" has been proposed in murine models (8). Whether these paradigms translate to human tumor biology remains unanswered. Critical species-specific differences in both innate and adaptive immunity make assumptions of equivalence unwise (9), especially given recent studies that have shown that certain rodent models poorly replicate inflammatory diseases in humans (10). In humans, correlative studies using immunohistochemistry have shown that TAN infiltrates are associated with a poor prognosis for patients with head and neck cancer (11), renal cell carcinoma (12), melanoma (13), hepatocellular cancer (14), and colon cancer (15). In contrast, high tumor neutrophil counts have been associated with a favorable outcome for patients with gastric cancer (16). The results in lung cancer have been divergent (17, 18). To our knowledge, there have been no reports regarding the functional role of TANs in the progression of human cancers. Thus, one goal of this work was to determine the phenotype and function of TANs in early-stage lung cancer using fresh surgically obtained tumor.

A major challenge in TAN biology is deciphering the complex interaction of activated neutrophils with T cells in the tumor microenvironment. Understanding the role of TANs in regulating T cell responses in cancer patients is particularly important because cytotoxic T lymphocytes are the chief effector cells mediating antigen-driven antitumor immunity. There is evidence that activated neutrophils can interact with T cells in dichotomous ways. Several studies have shown that neutrophils can present antigens
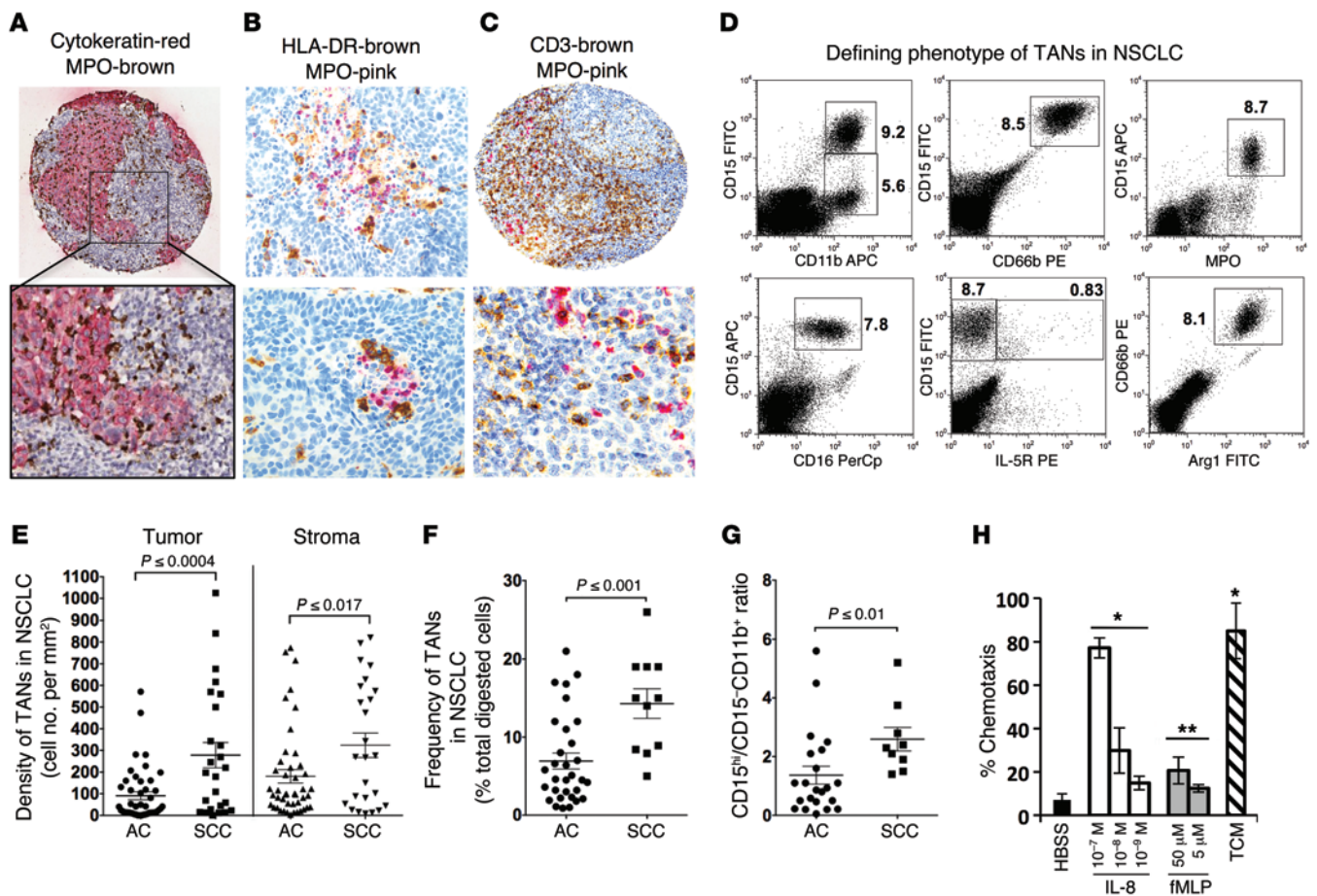
Figure 1. Neutrophils infiltrate NSCLC tissue. (**A–C**) Lung cancer tissue sections were stained using 2-color immunohistochemistry for MPO, HLA-DR, and CD3 to visualize neutrophils, APCs, and T lymphocytes, respectively. Representative images are shown. Original magnification, ×10 (**A** and **C**, top), ×20 (**B**, top), ×40 (bottom). (**D**) Representative dot plots of total tumor cells that define the phenotype of TANs in NSCLC. TANs were defined as CD15hiCD66b+ CD11b+CD16intArg1+MPO+IL-5Ra−. Results represent 1 of 20 experiments. Numbers represent the percentage of TANs. (**E**) Comparative immunohistochemical analysis of TAN density (cells/mm²) in AC (*n* = 45) and SCC (*n* = 25) performed by counting of MPO+ cells in the tumor stroma and the tumor islets. Statistical analyses were performed with Student's *t* test for unpaired data. (**F**) The frequency of TANs in AC (*n* = 31) and SCC (*n* = 11) determined by flow cytometry as the percentage of CD11b+CD15hiCD66b+ cells among all cells in tumor. Cumulative results from 42 independent experiments are shown in the scatter plot. Student's *t* test for unpaired data. (**G**) The ratio of TANs to other CD15−CD11b+ cells in AC (*n* = 22) and SCC (*n* = 9). Mann-Whitney test for unpaired data. For all scatter plots, error bars represent mean ± SEM. (**H**) PBNs were analyzed for migration in the Neuro Probe ChemoTx system. Each experiment was run in triplicate and repeated at least 3 times. Results of 1 representative experiment are shown. Error bars represent mean ± SEM. Statistical analysis was performed with Kruskal-Wallis and Dunn's multiple comparison tests (*$P \leq 0.05$, **$P \leq 0.01$). fMLP, *N*-formyl-methionyl-leucyl-phenylalanine.

and provide accessory signals for T cell activation (19–22). Other studies have suggested that peripheral blood neutrophils (PBNs) can suppress antigen-nonspecific T cell proliferation through the release of arginase-1 and the production of ROS (23–25). To date, the suppressive function of granulocytic cells in cancer patients has generally been attributed to a circulating low-density granulocytic myeloid-derived suppressor cell (G-MDSC) population (26–28). However, there is some uncertainty about whether G-MDSCs exist in humans and whether they are simply a sequela of disease progression. Thus, given the unclear role of neutrophils in the regulation of T cell responses, a second major goal of this study was to determine the effects of TANs on T cell activation.

Results

Intratumoral neutrophils constitute a significant portion of infiltrating cells in lung cancers. To identify and localize TANs, sections

from tumor microarrays containing 45 adenocarcinomas (ACs) and 25 squamous cell carcinomas (SCCs) were double-stained for cytokeratin to identify tumor cells (red) and myeloperoxidase (MPO) to identify TANs (brown) (Figure 1A). The median numbers of MPO+ cells present in the tumor islets and stroma in AC (40 cells/mm² and 97 cells/mm², respectively) were significantly less ($P < 0.02$) than those seen in SCC (197 cells/mm² and 269 cells/mm², respectively) (Figure 1E).

Double staining of tumor sections with MPO and HLA-DR or CD3 revealed that neutrophils often colocalized with APCs (Figure 1B) and T cells (Figure 1C) throughout the lung tumor microenvironment. In some cases, TANs were more associated with microabscesses or coagulative necrosis (Figure 1B, top).

To perform a more detailed evaluation of TANs by multicolor flow cytometry, the generation of high-quality single-cell suspensions is required. We tested several commercially available
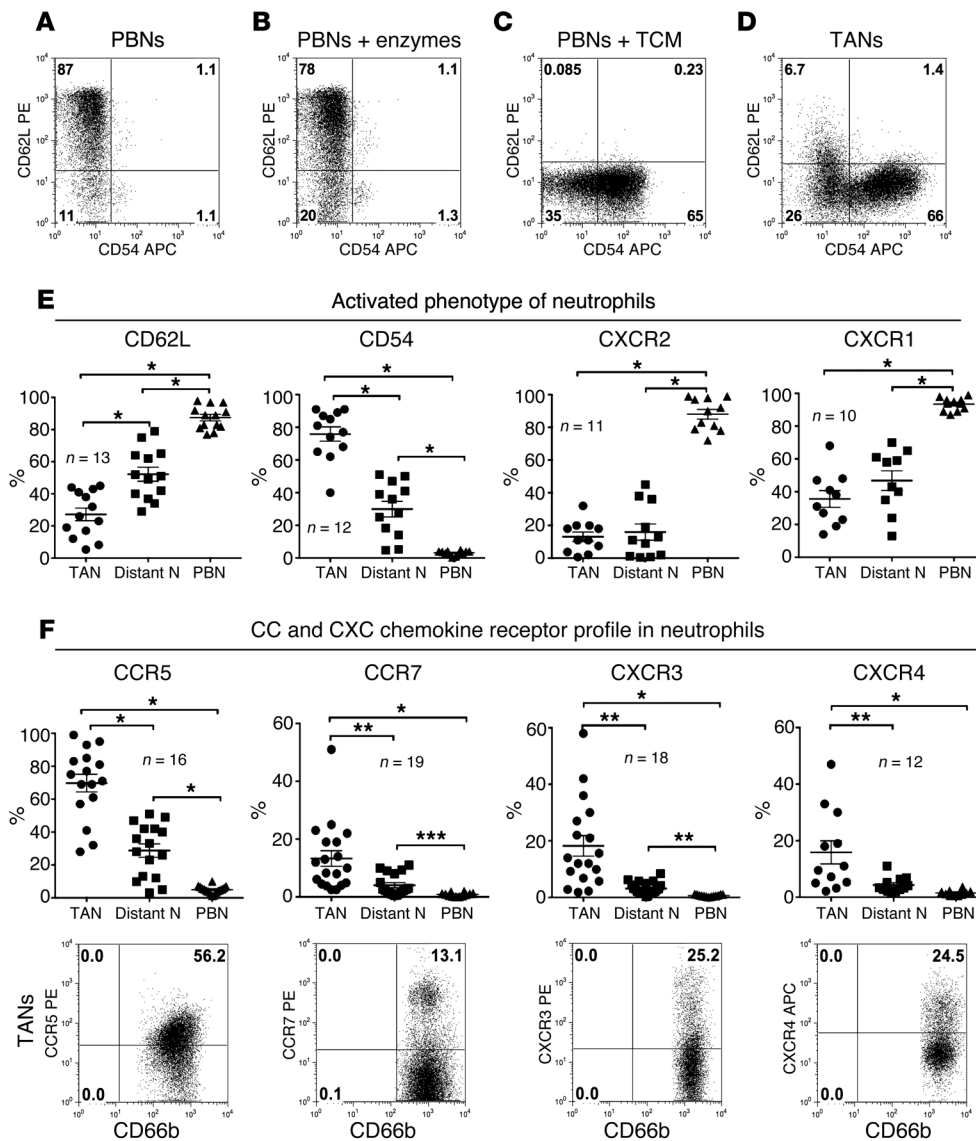
Figure 2. TANs acquire an activated phenotype and novel repertoire of chemokine receptors. (A) Expression of the activation markers CD62L and CD54 on CD15hiCD66b+ PBNs. PBNs were isolated from lung cancer patients using anti-CD15 beads. Results represent 1 of 5 experiments. **(B)** Digestion protocol did not elicit premature activation of resting PBNs. Results represent 1 of 5 experiments. **(C)** PBNs acquire an activated CD62LloCD54+ phenotype after treatment with TCM in plates with ultralow attachment surface. Each experiment was repeated at least 5 times. **(D)** A single-cell suspension was obtained from freshly harvested tumor tissues. TANs were gated on CD11b+CD15hiCD66b+ cells and further analyzed for the expression of activation markers. TANs displayed an activated CD62LloCD54+ phenotype. Results represent 1 of 12 experiments. **(E)** Expression of the activation markers on gated CD11b+CD15hi TANs, distant lung neutrophils (Distant N), and PBNs. **(F)** Expression of CCR5, CCR7, CXCR3, and CXCR4 was analyzed on gated CD11b+CD15hiCD66b+ TANs, distant lung neutrophils, and PBNs of cancer patients. Bottom: Representative dot plots. Numbers represent the percentage of cells in each quadrant. Top: Summary of all patient data. Error bars represent mean ± SEM. Statistical analyses were performed with repeated-measures 1-way ANOVA with Tukey's multiple comparison test for CD62L, CD54, CXCR2, CXCR1, and CCR5, and Kruskal-Wallis and Dunn's multiple comparison tests for CCR7, CXCR3, and CXCR4 ($*P \leq 0.001$, $**P \leq 0.01$, $***P \leq 0.05$).

and individually customized enzymatic cocktails to optimize cell yield, cellular viability, myeloid cell population recovery, preservation of myeloid cell surface marker expression, and induction of neutrophil activation (Supplemental Figure 1; supplemental material available online with this article; doi:10.1172/JCI77053DS1). We selected a combination cocktail (described in Methods) that was composed of several enzymes used at low concentrations and led to a high yield of viable single cells (Supplemental Figure 1, A and B) with minimal enzyme-induced ex vivo effects on neutrophil activation (Figure 2, A and B) and cleavage of myeloid and lymphoid cell markers (Supplemental Figure 1, C–G). Once optimized, we studied tumors from 86 non–small-cell lung carcinoma patients with stage I–II SCC and AC histology. The detailed patient characteristics are shown in Supplemental Table 1.

Single-cell suspensions from these fresh human lung tumors were stained for neutrophil markers (CD15, CD66b, MPO, and arginase-1 [Arg1]), myeloid lineage markers (CD11b, CD16, and CD33), and the eosinophil marker IL-5Rα, by flow cytometry. TANs were defined as CD15hiCD66b+CD11b+MPO+Arg1+CD16int

cells (Figure 1D). Importantly, the CD15hiCD66b+CD11b+ granulocytes had negligible expression of the eosinophil-associated surface marker IL-5Rα (Figure 1D). In multicolor tracings, we defined TANs as either CD15hiCD11b+ or CD66b+CD11b+, since there was a 100% concordance between CD15 and CD66b (Figure 1D).

The CD15hiCD11b+ TANs were found to be present in varying frequencies, ranging from 2% to 25% of live cells in the tumor microenvironment in all of the NSCLC studied (Figure 1F). In agreement with the immunohistochemical data (Figure 1E), the frequency of TANs and the CD15hiCD11b+ to CD15−CD11b+ ratio were significantly higher ($P = 0.001$) in patients with SCC (~15% of live cells; ratio of 2.6) compared with patients with an AC (~7% of live cells; ratio of 1.4) (Figure 1, F and G). This indicates that CD15hiCD11b+ TANs constituted the major proportion of CD11b+ tumor-infiltrating myeloid cells in patients with SCC. It is noteworthy that the proportion of TANs in tumor tissue of both histological types did not correlate with tumor size (Supplemental Table 2 and Supplemental Figure 5, A–C). Importantly, the density of intratumoral neutrophils was not associ-
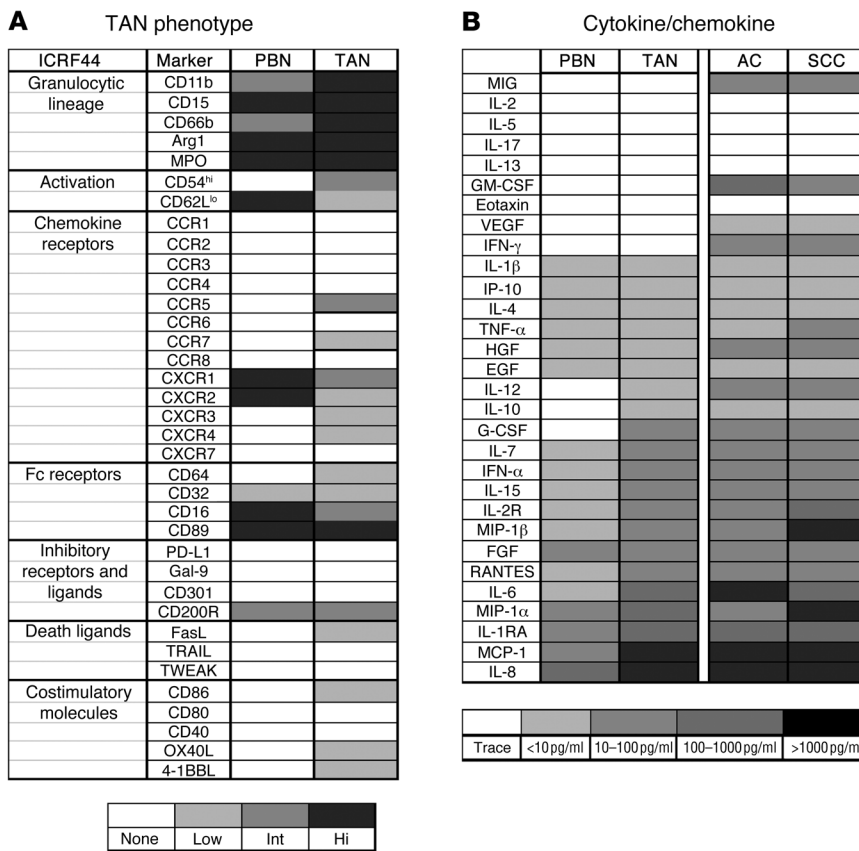
A   TAN phenotype

ICRF44	Marker	PBN	TAN
Granulocytic lineage	CD11b		
	CD15		
	CD66b		
	Arg1		
	MPO		
Activation	CD54hi		
	CD62Llo		
Chemokine receptors	CCR1		
	CCR2		
	CCR3		
	CCR4		
	CCR5		
	CCR6		
	CCR7		
	CCR8		
	CXCR1		
	CXCR2		
	CXCR3		
	CXCR4		
	CXCR7		
Fc receptors	CD64		
	CD32		
	CD16		
	CD89		
Inhibitory receptors and ligands	PD-L1		
	Gal-9		
	CD301		
	CD200R		
Death ligands	FasL		
	TRAIL		
	TWEAK		
Costimulatory molecules	CD86		
	CD80		
	CD40		
	OX40L		
	4-1BBL		

Intensity key: None | Low | Int | Hi

B   Cytokine/chemokine

	PBN	TAN	AC	SCC
MIG				
IL-2				
IL-5				
IL-17				
IL-13				
GM-CSF				
Eotaxin				
VEGF				
IFN-γ				
IL-1β				
IP-10				
IL-4				
TNF-α				
HGF				
EGF				
IL-12				
IL-10				
G-CSF				
IL-7				
IFN-α				
IL-15				
IL-2R				
MIP-1β				
FGF				
RANTES				
IL-6				
MIP-1α				
IL-1RA				
MCP-1				
IL-8				

Intensity key: Trace | <10 pg/ml | 10–100 pg/ml | 100–1000 pg/ml | >1000 pg/ml

Figure 3. Characterization of TANs. (**A**) Heat map comparing the phenotypes of TANs and PBNs. A single-cell suspension was obtained from freshly harvested tumor tissues, and expression of the indicated markers was assessed using flow cytometry. TANs were gated on CD11b⁺CD15ʰⁱ cells and further analyzed for the expression of indicated markers. PBNs were treated similarly to TANs. Expression of each marker was analyzed in 10–18 patients. The intensity key for the heat map is shown below. (**B**) The cytokine/chemokine production by TANs, PBNs, and total tumor dissociates of AC and SCC. TANs and PBNs were isolated from tumor tissues and peripheral blood of lung cancer patients (*n* = 5) using magnetic beads. Purified neutrophils and unseparated cells from digested tumor were cultured for 24 hours in the cell culture medium, and cell-free supernatants were collected and frozen. The indicated factors were detected using the Cytokine Human 30-Plex assay. The presence of each secreted factor was heat-mapped on the basis of the concentration in tested supernatants, as indicated below.

ated with smoking use in the patients (Supplemental Table 2 and Supplemental Figure 5D).

To determine whether the tumor microenvironment stimulates trafficking of neutrophils, resting PBNs were assayed for transwell migration in the presence of tumor-conditioned medium (TCM) collected from digested tumors. In this assay, we observed that TCM induced a strong chemotactic response in blood neutrophils (Figure 1H). In fact, TCM was as efficient as high concentrations of IL-8, a known neutrophil chemotactic factor, in attracting CD15⁺ granulocytes (Figure 1H).

Neutrophils are activated in the tumor microenvironment in patients with NSCLC. Since changes in cell adhesion molecules (CD62L, CD54) and CXC chemokine receptors (CXCR1, CXCR2) have been reported to correlate with leukocyte activation, augmented chemotaxis, and transendothelial migration (29, 30), these markers were measured on circulating and tumor-associated CD11b⁺CD15ʰⁱ neutrophils. There was no significant difference between lung cancer patients and healthy donors in the expression of these markers on PBNs; these neutrophils shared the phenotype of resting naive cells, i.e., CD62LʰⁱCD54⁻CXCR1ʰⁱCXCR2ʰⁱ (Figure 2, A and E).

Previously, others have described a distinct subset of activated CD11b⁺CD14⁻CD15⁺CD33⁺ low-density granulocytes in the PBMC fraction of patients with advanced stages of NSCLC (31). This population has been referred to as granulocytic myeloid-derived suppressor cells (G-MDSCs), because of their ability to suppress T cell proliferation (32). We analyzed PBMCs from 20 healthy donors and 20 lung cancer patients at early stages of disease for the presence of G-MDSCs and found that their frequency in cancer patients was low and not significantly different from the frequency in healthy donors (0.9% ± 0.17% and 0.7% ± 0.18%, respectively).

Next, we evaluated the expression of activation markers on CD11b⁺CD15ʰⁱ TANs and neutrophils isolated from lung tissue adjacent to the lung cancer (Distant N; Figure 2E). Notably, the digestion protocol did not elicit premature activation of resting PBNs (Figure 2B). In contrast to PBNs, CD11b⁺CD15ʰⁱ TANs markedly upregulated CD54 and downregulated CD62L, CXCR1, and CXCR2 (Figure 2, D and E), acquiring the phenotype of highly activated cells (CD62LˡᵒCD54⁺CXCR1ˡᵒCXCR2ˡᵒ). However, when resting PBNs were isolated from healthy donors and cultured in the presence of primary TCM, they rapidly acquired an activated CD62LˡᵒCD54ʰⁱ phenotype, suggesting that tumor-derived factors are sufficient to trigger these changes (Figure 2C). Similarly to TANs, neutrophils from distant noninvolved lung downregulated the expression of CXCR1 and CXCR2 when compared with PBNs. However, the analysis of the CD54 and CD62L expression demonstrated that distant neutrophils were less activated compared with TANs (Figure 2E). There were no differences in the expression of activation markers on TANs between patients with AC and SCC (Supplemental Table 2).

Phenotypic changes in tumor-infiltrating neutrophils. There is growing evidence that the inflammatory microenvironment may induce a novel chemokine receptor repertoire on infiltrating neutrophils that increases their functional responsiveness to surrounding chemokines (33). Thus, we determined whether neutrophils gained a new chemokine receptor expression profile in lung tumors.

Peripheral blood and tumor-associated CD11b⁺CD15ʰⁱCD66b⁺ neutrophils from patients with lung cancer were assayed for a wide

array of CC (CCR1–CCR7) and CXC (CXCR1–CXCR7) chemokine receptors. Subpopulations of TANs expressed CCR7, CXCR3, and CXCR4, whereas these chemokine receptors were absent on PBNs (Figure 2F and summarized in Figure 3A). Virtually all TANs expressed high levels of CCR5, which was absent on PBNs (Figure 2F). Interestingly, the proportion of CCR5-positive TANs was significantly higher in patients with AC compared with SCC ($P = 0.04$) (Supplemental Table 2). In addition, CXCR1 and CXCR2 were dramatically downregulated on TANs and distant neutrophils (Figure 2E). The expression of CCR5, CCR7, and CXCR3 on the distant neutrophils was significantly higher in comparison with PBNs ($P < 0.01$) and significantly lower in comparison with TANs ($P < 0.01$). These differences in chemokine receptor expression were consistent, regardless of whether they were measured by cell surface expression (MFI) or as a percentage of chemokine receptor–positive neutrophils. Importantly, there were no differences in the expression of CC and CXC receptors on PBNs between healthy donors and patients with stages I–II NSCLC (data not shown).

The activation of neutrophils has also been suggested to lead to the upregulation of inhibitory receptors and ligands that negatively regulate T cell responses (34–37). However, the expression of PD-L1, galectin-9, CD200R, and CD301 was not increased on TANs in 10 patients with early stages of AC or SCC (Figure 3A). In addition, we found that TANs expressed low levels of FasL and the FcRI receptor CD64 (albeit higher than PBNs), whereas the expression of the FcγRIII receptor CD16 was downregulated compared with that seen on PBNs (Figure 3A).

Engagement of CD15 or CD66b molecules in the isolation of TANs. Given studies that show minimal effects of positive selection of granulocytes by anti-CD15 Ab–conjugated magnetic microbeads on ROS production or phagocytosis (38), we used a combination of our tumor digestion protocol and anti-CD15 microbeads to isolate granulocytes from digested tumors and peripheral blood for functional studies. We first treated peripheral blood of healthy donors with the enzymatic cocktail, and then isolated neutrophils using anti-CD15 microbeads. Analysis of the expression of the activation markers CD62L and CD54 on PBNs indicated that these cells were not prematurely activated or adversely affected by this process (Figure 2, A and B). Using this approach, we found that isolation of TANs with the anti-CD15 microbeads yielded high neutrophil purity, as defined by the CD15^{hi}CD66b$^+$CD11b$^+$MPO$^+$Arg1$^+$ phenotype (Supplemental Figure 3A). We verified the cellular purity of TANs in every patient by flow cytometry and cytomorphology. TANs isolated with purity less than 90% were discarded. Over 95% of the sorted cells expressed the neutrophilic markers CD11b, MPO, CD66b, and Arg1. Cytospins were prepared from isolated TANs, and pathological review confirmed that the cytomorphology of these cells was consistent with granulocytes (Supplemental Figure 3D). Importantly, annexin V and propidium iodide (PI) staining of isolated CD15$^+$ PBNs showed that only 9% ± 3% of the cells were in apoptosis, indicating that significant cell death was not occurring during the isolation procedures (Figure 4, A and B). CD15^{hi}CD66b$^+$CD11b$^+$ TANs isolated from the majority of patients with lung cancer were MPO and Arg1 positive (Supplemental Figure 3, B and C). However, in some patients we found that the fraction of TANs had reduced intracellular MPO and Arg1, suggesting that these enzymes had already been

released in the tumor tissue before isolation. Isolation of TANs and PBNs using positive selection with engagement of CD66b demonstrated similar results (data not shown).

Cytokine/chemokine profile of TANs and total NSCLC cells. To describe the range of inflammatory factors secreted by neutrophils in lung cancer patients, 24-hour cell culture supernatants from purified TANs and PBNs were analyzed by a multiplexed fluorescent bead–based immunoassay. In addition, we analyzed these factors in the supernatants collected from total cells of digested AC or SCC. The heat map in Figure 3B shows that many chemokines and cytokines were upregulated in the TAN group. TANs isolated from patients with AC or SCC, compared with PBNs from the corresponding patients, had significantly increased ($P < 0.05$) production of the proinflammatory factors MCP-1, IL-8, MIP-1α, and IL-6 (Figure 3B). Importantly, TANs were able to simultaneously secrete considerably more of the antiinflammatory IL-1R antagonist compared with PBNs.

Interestingly, the analysis of cytokines secreted by digested tumors harvested from 5 patients with AC and 5 patients with SCC revealed a relative preponderance of the Th1 proinflammatory cytokines IFN-γ (100 ± 58 pg/ml), IL-12 (18 ± 4 pg/ml), and TNF-α (81 ± 27 pg/ml), compared with the Th2 cytokines IL-4 (2.6 ± 1.8 pg/ml), IL-5 (not detectable), IL-10 (9.8 ± 3 pg/ml), and IL-13 (not detectable) (Figure 3B). The concentration of the proangiogenic cytokine VEGF was extremely low (8 ± 2.7 pg/ml) in the supernatants from digested AC and SCC. Several prominent NSCLC-derived cytokines, such as IL-8, MCP-1, IL-1RA, GM-CSF, and MIG, were present in high quantities in the cell culture supernatants collected from total cells of AC and SCC. However, there were some significant differences ($P < 0.05$) in the cytokine production between the tumor types. Compared with AC, SCC had significantly increased secretion of MIP-1α, MIP-1β, TNF-α, and IL-2R. In contrast, AC produced significantly ($P < 0.05$) more IL-6 and GM-CSF. MIP-1α has been shown to promote neutrophil chemotaxis (39); therefore its increased production in SCC may explain the high number of TANs relative to AC (Figure 3B).

TANs exhibit high phagocytic activity, and the ability to generate ROS in vitro. To assess functionality, PBNs and TANs were isolated from the same cancer patient and evaluated for their ability to survive in culture, phagocytose bacteria, and produce ROS in vitro. There was no significant difference in the number of apoptotic cells in freshly isolated PBNs and TANs (5% ± 2.8% and 9% ± 3% of annexin V$^+$PI$^-$ and annexin V$^+$PI$^+$ cells, $P = 0.4$, respectively) (Figure 4A, top dot plots, and Figure 4B). After 20 hours in culture, there was no survival advantage for TANs compared with PBNs (Figure 4A, center dot plots, and Figure 4B). However, when either freshly isolated PBNs or TANs were cultured in the presence of TCM, these cells had substantially increased survival time compared with PBNs and TANs that were cultured in standard medium (Figure 4, A and B). About 40% of PBNs and TANs cultured in the presence of TCM were still viable at 48 hours (Figure 4B). These data suggest that tumor-derived factors prolong neutrophil survival in the tumor microenvironment.

Next, we examined the phagocytic activity of TANs and resting PBNs by measuring the uptake of red fluorescent pHrodo *E. coli* bioparticles. The results showed that TANs phagocytosed the bioparticles as efficiently as PBNs (Figure 4D). There was no
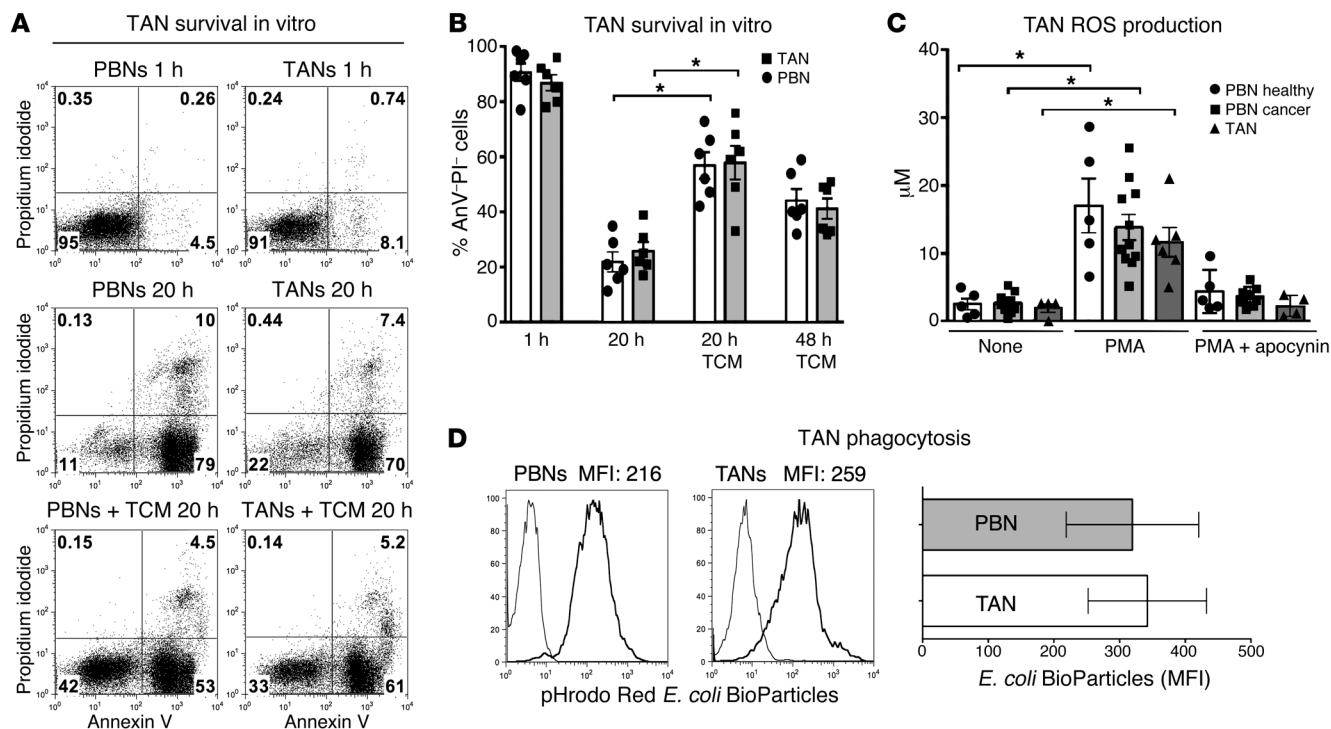
Figure 4. Characterization of neutrophils isolated from tumor tissues and peripheral blood of patients with NSCLC. (**A** and **B**) Neutrophil survival in vitro. TANs and PBNs were isolated from lung cancer patients with magnetic beads by positive selection. Cells were cultured in cell culture medium with or without TCM for 20 and 48 hours. TANs and PBNs were then assessed for apoptosis by FACS analysis of annexin V/PI staining at 1, 20, and 48 hours. Dot plots represent 1 of 6 similar experiments. Numbers represent the percentage of cells in each quadrant. Summary results from 6 lung cancer patients are also shown (*$P \leq 0.01$, Wilcoxon matched-pairs rank test). (**C**) Production of H_2O_2 in TANs and PBNs isolated from lung cancer patients and healthy donors was measured using Amplex Red with horseradish peroxidase. Error bars represent mean ± SEM from 5 independent experiments (*$P \leq 0.001$, Wilcoxon matched-pairs rank test). (**D**) Phagocytic capacity of TANs. TANs and PBNs were isolated and incubated with pHrodo Red *E. coli* BioParticles for 45 minutes to allow phagocytosis (internalized particles become fluorescent [red]). Histograms from 1 representative experiment are shown. Phagocytosis performed at 4°C and 37°C is shown by thin and thick lines, respectively; MFI values are as indicated in histograms. Summary results from 6 lung cancer patients are also shown (Wilcoxon matched-pairs rank test).

difference in the phagocytic activity between PBNs from cancer patients and healthy donors (data not shown).

We also quantified the spontaneous and PMA-stimulated ROS production by circulating and tumor-associated neutrophils using the Amplex Red assay. Despite the fact that TANs were activated, spontaneous ROS production was minimal and no different from that of resting PBNs from lung cancer patients or healthy donors (Figure 4C). However, the stimulation of PBNs and TANs with PMA resulted in a dramatic increase in H_2O_2 production, suggesting that TANs were not dysfunctional and could be stimulated further (Figure 4C). Mechanistically, ROS production in the neutrophils was mediated by the NADPH oxidase complex (NOX), since coculture of the TANs with the NOX inhibitor apocynin substantially decreased PMA-induced ROS generation (Figure 4C).

Together, our data on isolated TANs show that when appropriately triggered, they can perform major functions such as phagocytosis and ROS production, suggesting that they are not "exhausted" or hypofunctional.

Neutrophils from malignant and nonmalignant lung tissue stimulate antigen-nonspecific T cell proliferation. Multiple reports suggest that MDSCs in human and murine tumors are partially composed of granulocytic cells, and that these populations tend to negatively modulate effector T cell functions (27, 40). Accord-

ingly, we measured the effect of TANs on lymphocyte proliferation in a CFSE-based T cell suppression assay. First, in order to validate this assay in our hands, we isolated Tregs (effectors) from the peripheral blood of lung cancer patients and cocultured them with CFSE-labeled healthy donor PBMCs (responders) that had been stimulated with plate-bound anti-CD3 Abs. As expected, after 4 days, we found that the proliferation of both CD4+ and CD8+ T cell populations exposed to Tregs was markedly suppressed compared with that of control cells (Supplemental Figure 2A).

Next, we performed similar experiments in which PBNs or TANs (effectors) were isolated from cancer patients and cocultured with healthy donor PBMCs (responders) that had been stimulated with plate-bound anti-CD3 Abs. We found that the proliferation of stimulated T cells after 4 days was not altered by exposure to PBNs (Figure 5A). Surprisingly, when the stimulated PBMCs were cocultured with TANs, the proliferation of CD4+ and CD8+ cells was markedly augmented. Specifically, whereas approximately 50% of control T cells were CFSE^{lo} and underwent 1–6 rounds of cell division, the dividing T cell fraction significantly increased (to as much as 95%) in the presence of TANs (Figure 5A).

Isolation of TANs and PBNs using positive selection with engagement of the CD66b molecule demonstrated similar results (Supplemental Figure 2C). To confirm that our results were not
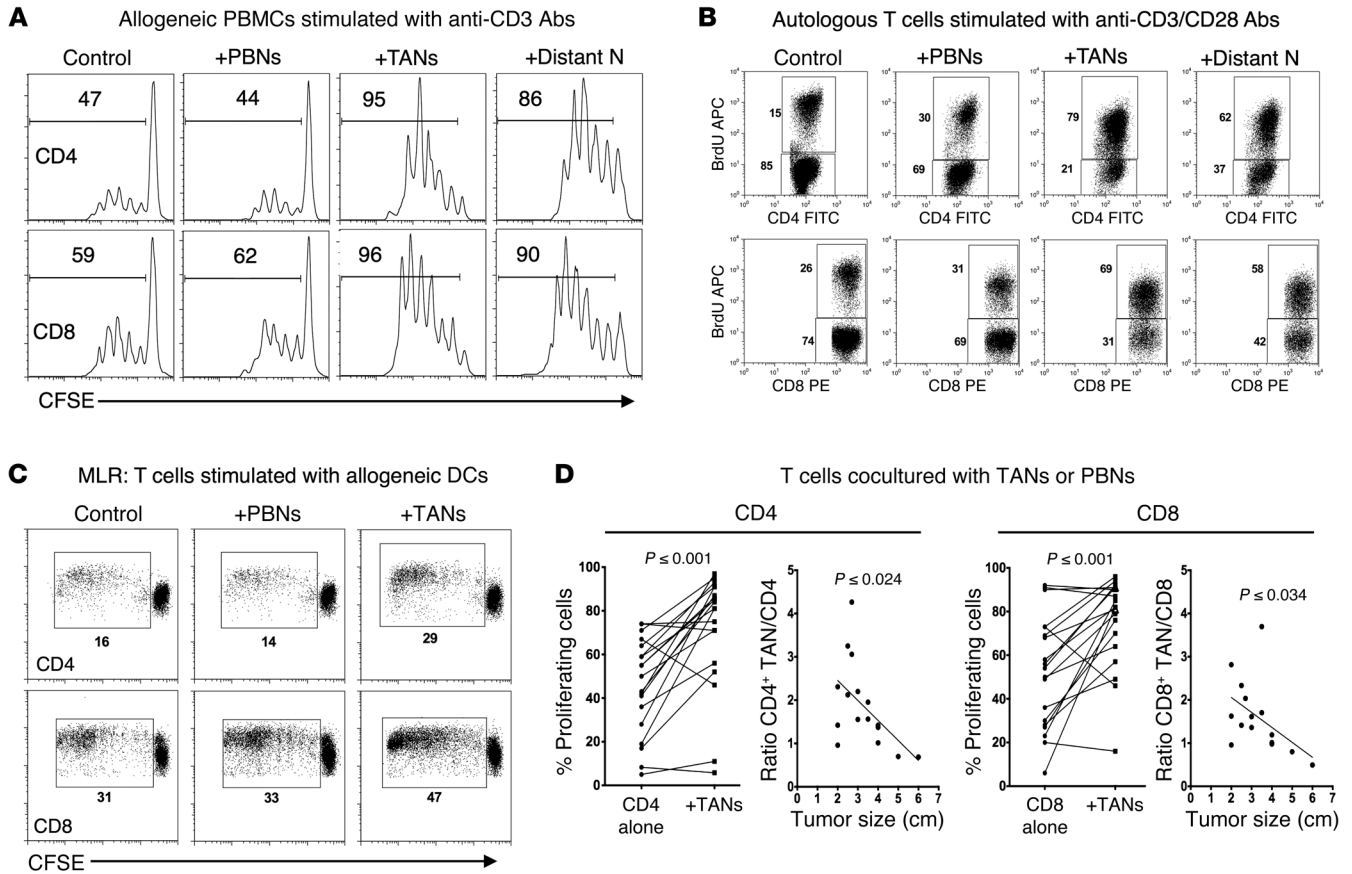
Figure 5. T cell proliferation in the presence of TANs or PBNs. (**A**) CFSE-labeled PBMCs isolated from a healthy donor were stimulated with plate-bound anti-CD3 Abs and mixed with TANs, neutrophils from distant lung tissue, or PBNs isolated from cancer patients at a 1:1 ratio for 4 days. Representative results from 1 of 12 experiments are shown. Numbers on histograms represent the percentage of proliferating T cells. (**B**) Autologous T cells were purified from PBMCs, stimulated with plate-bound anti-CD3 Abs and anti-CD28 Abs, and cultured alone or with PBNs, distant neutrophils, or TANs. 72 hours later, proliferation of T cells was assessed by incorporation of BrdU into DNA. Representative results from 1 of 5 experiments are shown. (**C**) Mixed lymphocyte reaction (MLR). CFSE-labeled T cells isolated from PBMCs of healthy donors were stimulated with allogeneic DCs in the absence or presence of PBNs or TANs for 5 days. Representative results from 1 of 5 experiments are shown. Numbers on dot plots represent the percentage of proliferating T cells. (**D**) Change in percentage of proliferating CFSE^{lo} CD4$^+$ and CD8$^+$ cells cultured alone versus cells cultured in the presence of TANs (Student's t test, paired parametric test). Autologous PBMCs were stimulated with plate-bound anti-CD3 Abs and mixed with TANs at a 1:1 ratio for 4 days. Scatter plots show the correlation between tumor size and stimulatory activity of TANs defined as the ratio CFSE^{lo} (T cells +TANs)/CFSE^{lo} (T cells) (nonparametric Spearman correlation). Cumulative results from 16 independent experiments are presented.

due to contamination of our TANs by other tumor-infiltrating cells that may have escaped magnetic bead separation, we repeated the experiments using purified CD45$^+$CD11b$^+$CD15^{hi}CD66b$^+$ TANs collected by FACS. In triplicate experiments, the TANs sorted by flow cytometry again showed remarkable stimulatory effects on T cell proliferation (Supplemental Figure 2C).

To ensure that this stimulatory effect was not dependent on the allogenicity between healthy donor responders and patient TANs, or some artifact of the CFSE system, we repeated the T cell proliferation assay using T cells, PBNs, and TANs all isolated from the same patient. A BrdU incorporation assay demonstrated that the majority of T cells (79% of CD4$^+$ and 69% of CD8$^+$ cells) cocultured with TANs were in S phase of the cell cycle by 72 hours after stimulation, compared with only about 15%–30% of control T cells or T cells cocultured with PBNs (Figure 5B). This short-term assay revealed that activated T cells begin to actively synthesize DNA in the presence of TANs by 48 hours after stimulation compared

with control T cells or T cells cocultured with PBNs (Supplemental Figure 2E). Interestingly, in this experiment, we found that PBNs and TANs partially liberated Arg1 in the presence of activated T cells (Supplemental Figure 3E). However, the presence of arginase did not seem to affect the rate of T cell proliferation. These data support other studies showing that the arginase, which is liberated following spontaneous polymorphonuclear neutrophil death, is not sufficient for T cell suppression (41).

Neutrophils isolated from distant nonmalignant lung tissue were also able to stimulate allogeneic and autologous T cell proliferation (Figure 5, A and B). However, there was no significant difference in stimulatory activity of distant neutrophils when compared with TANs (Supplemental Figure 2D). This suggests that stimulatory capacity of distant neutrophils is a lung tissue–specific characteristic that might be driven by adjacent early-stage lung tumor.

In order to quantify the extent to which TANs are able to increase T cell proliferation, we mixed TANs with autologous
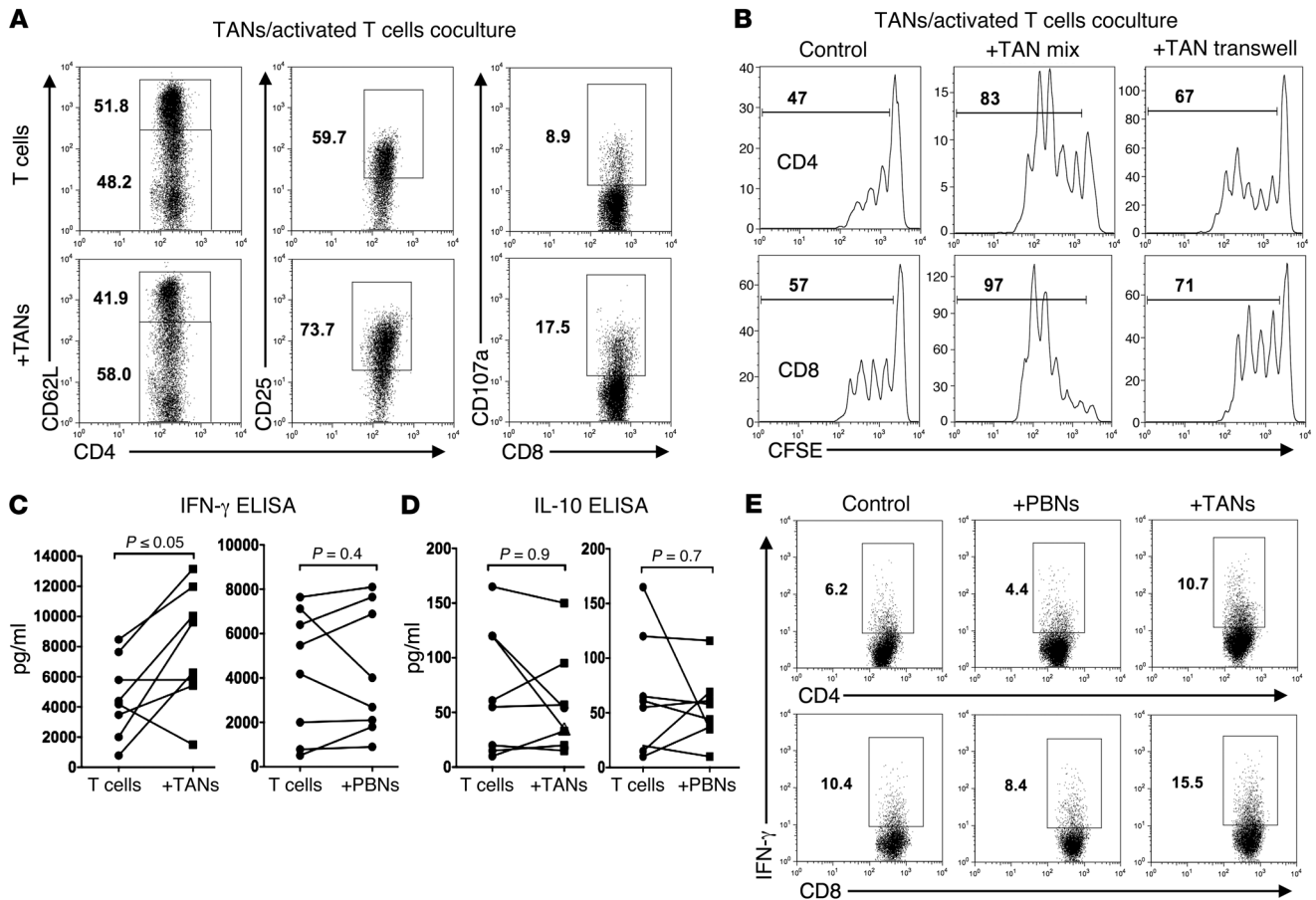
Figure 6. Effect of TANs on T cell activation, cytokine production, and proliferation. In all experiments, T cells were stimulated with plate-bound anti–CD3/CD28 Abs and incubated with TANs at a 1:1 ratio. (**A**) Expression of the CD62L, CD25, and CD107a markers on activated autologous T cells cultured with TANs for 20 hours. Representative dot plots from 1 of 3 experiments are shown. Numbers represent the percentage of CD4+ and CD8+ cells. (**B**) Flow cytometric analysis of autologous T cell proliferation in the presence of TANs using a transwell system. Activated CFSE-labeled T cells were mixed with TANs at a 1:1 ratio (TAN mix). To separate T cells and TANs, activated T cells were cultured in the bottom chamber and TANs were placed in the top chamber of the 24-well flat-bottom transwell culture plate (TAN transwell). Representative results from 1 of 3 experiments are shown. Numbers on histograms represent the percentage of proliferating T cells. (**C** and **D**) IFN-γ (**C**) and IL-10 (**D**) were measured by ELISA in 48- or 96-hour supernatants collected from cocultures of activated T cells with TANs or PBNs. Summary results from 8 lung cancer patients are shown in the graph (Wilcoxon matched-pairs rank test). (**E**) The percentage of IFN-γ– and IL-10–producing T cells cultured with TANs or PBNs was measured by intracellular cytokine staining at 48 hours of stimulation. The dot plots represent 1 of 3 independent experiments. Numbers represent the percentage of CD4+ and CD8+ cells.

PBMCs that had been stimulated with different concentrations of anti-CD3 Abs (Supplemental Figure 2B). Four days later, TANs dramatically increased the proliferation of CD4+ T cells from 15% to 64% ($P < 0.01$) and that of CD8+ T cells from 12% to 61% ($P < 0.01$). Moreover, the coculture of TANs with highly activated T cells (anti-CD3 Abs, 2.5 μg/ml) resulted in even more rapid division of these T cells.

Since the CD3/CD28–stimulated T cell response involves a robust polyclonal T cell proliferation, we investigated the ability of TANs and PBNs to modulate more physiological T cell responses induced by allogeneic DCs in a mixed-lymphocyte reaction. Allogeneic T cells (responders) were purified from the peripheral blood of healthy donors and cocultured with irradiated, mature, monocyte-derived DCs (MoDCs) (inducers) from unrelated donors. TANs or PBNs from patients with stage I–IIB lung cancer were added to the DCs as "third-party cells." Five days later, we found that inclusion of TANs resulted in an increased T cell proliferation that had been initiated by allogeneic MoDCs, compared

with control experiments (Figure 5C). These experiments were repeated with TANs from 5 patients with early-stage lung cancer. By day 5, the addition of TANs increased the proliferation of T cells 1.7- to 2.8-fold compared with PBNs. The TANs did not appear to preferentially increase CD4+ versus CD8+ T cell expansion.

Next, we asked whether treatment of PBNs with TCM would recapitulate the ability of TANs to stimulate T cell proliferation. We exposed PBNs from healthy donors to a variety of TCMs collected from digested AC or SCC. The majority of these TCMs prolonged survival time of PBNs up to 48 hours (Figure 4B) and induced the expression of the activation marker CD54 on the surface of PBNs (Figure 2C). However, TCM-treated PBNs were not able to stimulate T cell proliferation to a significant level (Supplemental Figure 3H). This indicates that short-term exposure of mature PBNs to tumor-derived factors is not sufficient to convert PBNs into stimulatory cells.

In total, we analyzed the effect of TANs on the proliferation of T cells from 16 patients with lung cancer. Overall, TANs sig-
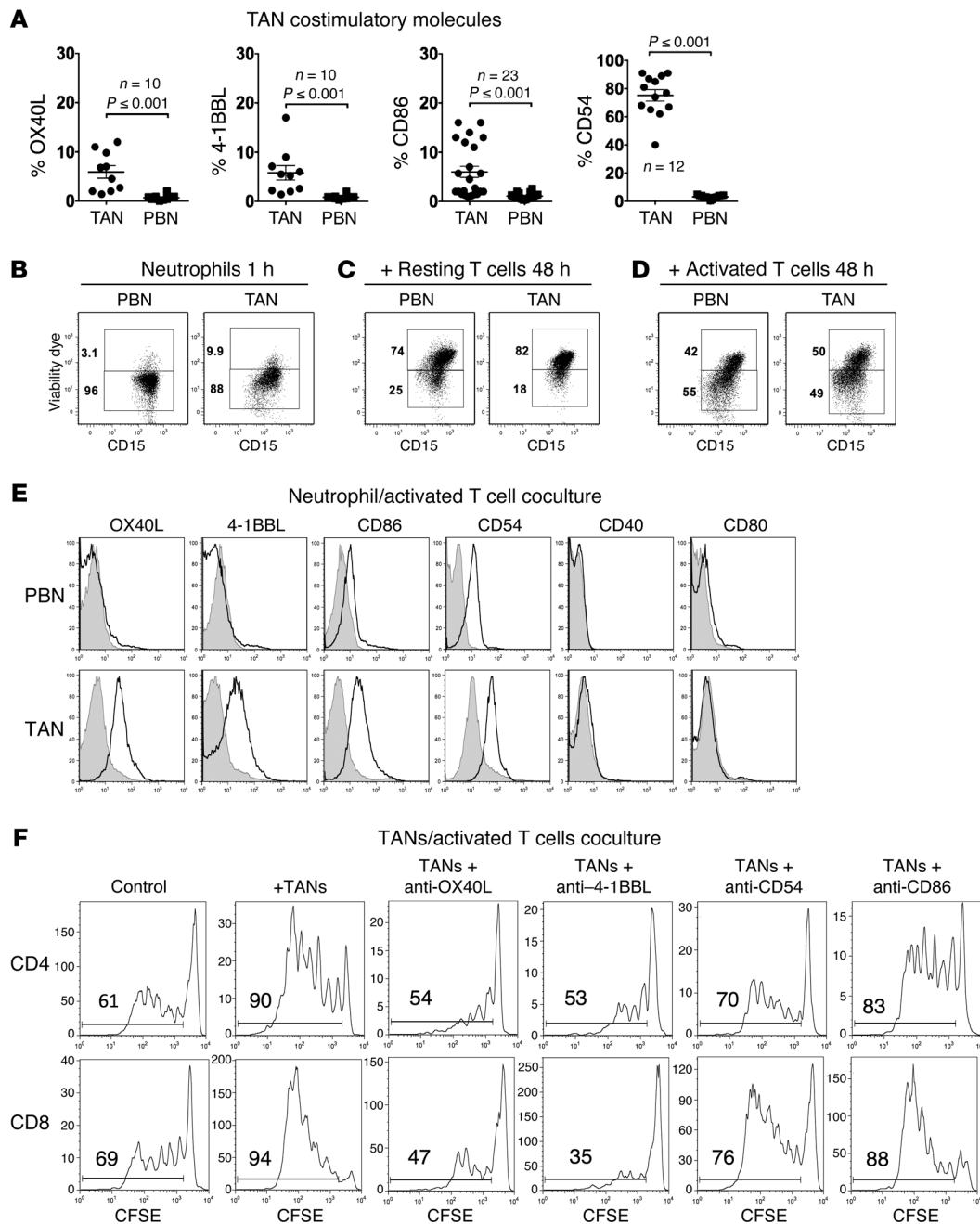
Figure 7. The expression of costimulatory molecules on TANs and their role in stimulation of T cell proliferation. (**A**) The expression of the costimulatory molecules on gated CD11b⁺CD15ʰⁱ TANs and PBNs was analyzed by flow cytometry. The top panel summarizes the data for all the patients. Error bars represent mean ± SEM. Statistical analyses were performed with Student's *t* test for paired data. (**B**–**D**) Neutrophil survival in the cell culture. Zombie Yellow Fixable Viability dye was used to discriminate viable CD15 neutrophils cultured alone (**B**) or in the coculture with resting T cells (**C**) and CD3/CD28–activated T cells (**D**). Representative dot plots from 1 of 5 experiments are shown. For all dot plots, numbers represent the percentage of cells in each quadrant. (**E**) The expression of costimulatory molecules was analyzed by flow cytometry on gated live CD11b⁺CD15ʰⁱ PBNs (top) and TANs (bottom) after 2 days of coculture with activated (black histograms) or resting autologous T cells (gray histograms). Results from 1 of 5 representative experiments are shown. (**F**) The efficacy of blocking Abs in ablating the stimulatory effect of TANs on T cell proliferation. Autologous PBMCs were stimulated with plate-bound anti-CD3 Abs and mixed with TANs at a 1:1 ratio in the presence or absence of blocking Abs against the indicated receptors for 4 days. Numbers on histograms represent the percentage of proliferating cells. Mouse IgG1 Abs were used as isotype control Abs in the control group. Results from 1 of 3 representative experiments are shown.

nificantly increased the proliferation of both CD4⁺ and CD8⁺ T cells an average of 2.1-fold (range 1.4- to 9-fold) compared with PBNs (Figure 5D; *P* = 0.001). Interestingly, as shown in Figure 5D and Supplemental Table 2, correlation analysis revealed that the

majority of TANs from larger tumors were associated with a lower capacity to augment T cell proliferation than TANs from smaller tumors. We also divided lung cancer patients into 2 groups: patients with small tumors (<3 cm, *n* = 7) and patients with large tumors

(>3 cm, $n = 9$). The analysis of these 2 groups using a Mann-Whitney nonparametric test also revealed that stimulatory activity of TANs from small tumors was significantly higher than that of TANs from large tumors (Supplemental Table 2). Interestingly, there were no significant associations between stimulatory activity of TANs and histological type of tumor, tumor stage, and smoking history (Supplemental Table 2 and Supplemental Figure 4, A–C).

TANs enhance T cell activation. To further examine the crosstalk between activated T cells and neutrophils in lung cancer patients, we assayed T cell activation and the capacity of activated T cells to produce cytokines in the presence of TANs or PBNs. T cell activation was assessed within 24 hours of exposure to anti-CD3/anti-CD28 Abs. When T cells were cultured with TANs, they more markedly upregulated CD25 (65% ± 11% vs. 41% ± 17%, $P = 0.001$) and downregulated CD62L (39% ± 14% vs. 54% ± 11%, $P = 0.01$), compared with control T cell populations. A representative experiment depicted in Figure 6A (left and center columns) demonstrates the effect of TANs on the expression of these markers in activated T cells. TANs did not affect CD69 expression on activated T cells (data not shown). We also found that the percentage of activated CD8+ cells expressing the lysosomal marker CD107a (LAMP-1) on the surface was twice as high in TAN/T cell cocultures compared with cultures of control T cells alone (Figure 6A, right column). Together, these data suggest that TANs tend to promote activation of T cells and degranulation of their cytotoxic granules.

The expression of CD25 also defines a distinct population of CD4+ FOXP3+ Tregs with suppressive activity in vitro and in vivo (42). However, after coculture for 4 days, analysis of FOXP3 expression showed no difference in activated CD4+ cells cultured with or without TANs (4.5% ± 1.1% and 5% ± 1.5%, respectively, $P > 0.05$) (Supplemental Figure 3F).

We also determined whether TANs or PBNs modulated the production of key Th1 or Th2 cytokines in activated T cells. For these experiments, we mixed TANs or PBNs with autologous CD3/CD28–stimulated T cells purified from peripheral blood of patients with NSCLC and quantified IFN-γ and IL-10 in the supernatants 96 hours later. Figure 6C demonstrates that TANs significantly increased IFN-γ production by activated T cells, as TAN/T cell cocultures had a much higher concentration of IFN-γ compared with T cells cultured alone ($P = 0.02$). PBNs isolated from lung cancer patients did not affect the IFN-γ production by activated T cells. Intracellular staining revealed a significant increase in the frequency of IFN-γ–positive CD4+ and CD8+ cells in the coculture with TANs compared with activated T cells cultured alone (Figure 6E). While the percentage of IFN-γ–producing T cells was slightly changed, the stimulation of T cell proliferation by TANs resulted in a larger number of T cells and increased overall cytokine levels in the supernatant after 4 days of coculture. In addition, there was no significant difference in the production of IL-10 by activated T cells cultured with TANs or PBNs (Figure 6D). Intracellular IL-10 was not detected in activated T cells cultured in the presence or absence of TANs and PBNs (data not shown).

Direct cell contact between TANs and T cells is important for T cell stimulation. In order to understand the primary mechanism of TAN/T cell effects, we investigated whether direct cellular contact was necessary for TANs to stimulate T cell proliferation, using a transwell assay system that separated the TANs or PBNs from

the T cells. The PBNs isolated from healthy donors or lung cancer patients did not induce the stimulation of T cell proliferation when the cells were mixed or separated (data not shown). When in direct contact, TANs induced a much higher level of T cell proliferation than in the transwell system, in which TANs were physically separated from activated T cells (Figure 6B). These data indicate that cellular contact is likely the chief mechanism by which TANs augment T cell proliferation. However, the TANs isolated from several patients demonstrated some stimulatory effect on T cells even when the cells were separated, suggesting that secreted factors are also involved in the stimulation of T cell proliferation, but to a lesser extent (Figure 6B, right column).

Expression of costimulatory molecules on TANs and their role in the stimulation of T cell proliferation. Given that the strong stimulatory effect of TANs on T cell proliferation was dependent on direct cell contact, we quantified the expression of costimulatory molecules (CD86, CD80, CD40, CD54 [ICAM-1], CD252 [OX40L], and CD137L [4-1BBL]) on the surface of TANs and PBNs by flow cytometry (Figure 7A). Circulating PBNs had minimal to no expression of these costimulatory molecules in all patients. The expression of CD54 was highly increased on the surface of TANs versus PBNs (75% ± 15% vs. 3% ± 1%, $P < 0.001$) (Figure 7A). In addition, we found moderate but statistically significant upregulation of CD86, OX40L, and 4-1BBL on the surface of TANs but not PBNs ($P < 0.001$). Figure 7A demonstrates that the expression of these markers varied widely from 0.5% to 20% among all cancer patients. However, the differences in the expression of these costimulatory molecules on TANs were not significantly correlated with tumor type, size, or stage (Supplemental Table 2 and Supplemental Figure 4, E–H). We were not able to detect the expression of CD80 or CD40 markers on the surface of TANs.

Given that TANs enhance the activation of T cells during cell coculture, we examined whether activated T cells, in turn, upregulate the expression of costimulatory molecules in TANs to further bolster their own proliferation. To test this hypothesis, we activated T cells with plate-bound anti–CD3/CD28 Abs and mixed them with autologous TANs or PBNs. Two days later, flow cytometry was used to characterize the viability of neutrophils cocultured with activated T cells and expression of costimulatory molecules on gated live CD11b+CD15+ TANs. Flow cytometry revealed that in the presence of activated T cells, the TANs and PBNs survived longer than neutrophils cultured with resting T cells (Figure 7, B–D). The activated T cells increased the lifespan of TANs and PBNs to 4 days (Supplemental Figure 3G). Importantly, TANs cocultured with activated T cells markedly upregulated OX40L, 4-1BBL, CD54, and CD86 costimulatory molecules, whereas PBNs increased expression of only CD86 and CD54 (Figure 7E). These data suggest that a preexisting activated state of TANs or some enhanced plasticity is required for subsequent T cell–induced upregulation of these costimulatory molecules. CD80 and CD40 continued to show low levels of expression on PBNs and TANs following exposure to activated T cells.

Next, we investigated the functional significance of these costimulatory molecules. In 3 experiments, TANs and CFSE-labeled activated autologous T cells were cocultured in the presence of blocking Abs against these upregulated costimulatory molecules. Figure 7F shows a representative experiment (all 3 showed the same results)

where the stimulatory effect of TANs was partially abrogated in the presence of anti-CD54 and -CD86 blocking Abs (right columns). The most pronounced effect was observed when anti-OX40L or anti–4-1BBL blocking Ab was added to the T cell/TAN coculture. These Abs completely blocked the strong stimulatory activity of TANs (Figure 7F, center columns). Notably, in the control groups, the proliferation of T cells without TANs was not affected by the presence of any of these blocking Abs. These data suggest that TANs enhance T cell proliferation by direct cell-cell signaling, likely due to the OX40L/OX40 and 4-1BBL/4-1BB pathways. Both pathways appear equally important for T cell proliferation.

Taken together, these results suggest that there is ongoing cross-talk between activated T cells and TANs that results in dramatic upregulation of costimulatory molecules on the surface of TANs, which enhances T cell proliferation. This interaction between the innate and adaptive sides of the immune system requires direct cell-cell interactions due to receptor engagement, although secretory cytokines may have a limited role in this relationship.

Discussion

This study provides a comprehensive phenotypic and functional characterization of tumor-infiltrating neutrophils in early-stage lung cancer patients. Our key observations were that TANs represented a significant proportion of the cellular composition of human lung tumors and that, in contrast to our expectations, early-stage lung cancer TANs were not hypofunctional or immunosuppressive, but were able to stimulate T cell responses.

Our data show that TANs express a "classic" activated phenotype characterized by upregulation of the adhesion molecule CD54 (ICAM-1) and downregulation of CD62L (L-selectin), CXCR1, CXCR2, and CD16 (29, 30). Another major change in the infiltrating neutrophils compared with systemic PBNs was in chemokine receptor expression, including upregulation of CCR5, CCR7, CXCR3, and CXCR4, and downregulation of CXCR1 and CXCR2. It has been suggested that the acquisition of new chemokine receptors by neutrophils at inflammatory sites expands their functional profile (33); however, the exact role of the chemokine receptors expressed on TANs is still unknown, and further studies are required to understand their functional significance.

In this study, we also characterized the phenotype of neutrophils from the nonmalignant lung tissue to demonstrate which characteristics of TANs are specific for the tumor microenvironment and which simply reflect the differences between blood and lung tissue neutrophils. Neutrophils from distant tissue versus TANs were more similar to each other than to blood neutrophils. However, we found that TANs exhibit an even more activated phenotype compared with neutrophils isolated from "distant" noninvolved lung tissue. The level of CCR5, CCR7, CXCR3, and CXCR4 expression on distant neutrophils was intermediate between those of PBNs and TANs. Although these data are interesting, there are some caveats associated with comparison of neutrophils from tumor and distant lung tissue. First, we believe the surrounding nonmalignant lung tissue is likely to be influenced by the adjacent tumor, so neutrophils infiltrating the adjacent lung tissue may not have exactly the same function and phenotype as those infiltrating normal lung tissue. Second, compared with tumor-infiltrating neutrophils, the majority of lung neutrophils likely represent a pool of marginated neutrophils (cells that are adherent to the endothelium of blood vessels of lung tissue) and neutrophils from alveolar space, making them difficult to define as tissue-specific.

In addition to changes in activation, we also found that the tumor microenvironment stabilizes and prolongs the survival of infiltrating neutrophils. In the presence of tumor-conditioned medium (TCM) rich in proinflammatory factors, such as IFN-γ, IL-6, IL-8, and GM-CSF (Figure 4B), TANs and naive blood neutrophils developed a significant survival advantage compared with control neutrophils. This is likely due to the ability of these proinflammatory factors to prolong the lifespan of human neutrophils by delaying apoptosis (43, 44).

Once TANs are activated in the tumor microenvironment, they appear to add to the complexity of the inflammatory milieu and are likely involved in the attraction of other leukocytes. TANs secreted large quantities of IL-8 in cell culture, which has been found to self-promote neutrophil survival and recruit more neutrophils. We also found that TANs released various immunoregulatory cytokines, chemokines, and growth factors, such as the proinflammatory mediators CCL2 (MCP-1), IL-8, CCL3 (MIP-1α), and IL-6, as well as the antiinflammatory cytokine IL-1RA. On the other hand, TANs can secrete factors that could be protumorigenic. MIP-1α may act as a growth, survival, and chemotactic factor for tumor cells (45). In our study, we did not see high levels of proangiogenic VEGF, but there were other growth factors that might support angiogenesis, such as FGF, HGF, and EGF.

Over the last decade, there has been an increasing focus on the interactions between myeloid cells and T cells in tumor-bearing mice. Most of these studies have focused on MDSCs and TAMs. The vast majority of the data suggest that these cells inhibit T cell proliferation and function (46–49). With regard to TAMs, the current paradigm is that these cells are primarily tumor-promoting (M2-type) cells but, under certain conditions, can be reprogrammed into tumor-inhibitory (M1-type) cells with therapeutic potential (50–52). Much less is known about murine TANs; however, work by our group (8) and others (5, 53–55) suggests that a similar N1 (antitumor) and N2 (protumor) polarization exists, and that most advanced tumors harbor N2-like TANs. Given this framework, we anticipated human TANs would inhibit T cell responses in human lung tumors. Unexpectedly, however, freshly isolated TANs from early-stage lung cancer patients did not suppress IFN-γ production or proliferation of T cells that had been activated with anti–CD3/CD28 Abs or allogeneic DCs. Instead, TANs increased T cell IFN-γ production and activation, and dramatically amplified T cell proliferation. Direct cell-cell contact was important for the neutrophil-mediated stimulation of T cell proliferation. One important feature of this interaction was cross-talk and mutual cell activation. With coculture, T cells further upregulated activation markers and produced more IFN-γ, whereas TANs upregulated the costimulatory molecules CD86, CD54, OX40L, and 4-1BBL. These molecules are not constitutively expressed on the surface of circulating neutrophils; however, they can be rapidly translocated from cytoplasmic granules onto the surface of neutrophils or be synthesized de novo under the appropriate circumstances (19, 56).

Follow-up experiments using blocking Abs against various costimulatory molecules showed that the OX40L/OX40 and 4-1BBL/4-1BB pathways were critical in TAN-mediated augmen-

tation of T cell proliferation. 4-1BBL/4-1BB and OX40/OX40L represent a pair of costimulatory molecules critical for T cell proliferation, survival, cytokine production, and memory cell generation, as well as reverse signaling for further activation of APCs (57, 58). Typically, the costimulatory molecules 4-1BBL and OX40L are expressed on APCs, including mature DCs, activated macrophages, and B cells (57). Our data suggest that the 4-1BBL and OX40L costimulatory molecules can also be upregulated on activated TANs as a result of the interaction with activated T cells. Thus, the OX40L/OX40 and 4-1BBL/4-1BB pathways have the potential to enhance antitumor immunity and break tumor-induced immune suppression and immunological tolerance. Furthermore, costimulation through 4-1BBL/4-1BB protects T cells from activation-induced cell death and enhances the antitumor effector functions of CD8+ melanoma tumor–infiltrating lymphocytes (59, 60).

Our data are consistent with previous studies showing that granulocytes can provide accessory signals for T cell activation (19, 21, 22). For instance, Radsak et al. reported that human circulating neutrophils are accessory cells for T cell activation after treatment with IFN-γ and GM-CSF (19). They found that neutrophil-dependent T cell proliferation could be partially inhibited by blocking Abs against MHC class II, CD86, and CD54. Interestingly, our findings showed that lung tumors were able to produce IFN-γ and GM-CSF, as well as to induce expression of CD86 and CD54 costimulatory molecules in TANs. However, blocking CD86 did not substantially inhibit the stimulatory capacity of TANs compared with blocking OX40L or 4-1BBL. Inhibiting CD54 resulted in partial ablation of this effect.

Our data are consistent with some literature showing the antitumor potential of neutrophils during tumor growth in some models (61–63). For instance, Suttmann and colleagues demonstrated that polymorphonuclear neutrophils are an indispensable subset of immunoregulatory cells and orchestrate T cell chemotaxis to the bladder during bacillus Calmette-Guérin immunotherapy (64). Augmentation of T cell proliferation and/or survival by tumor-infiltrating neutrophils was found to be critical in the establishment of antitumor immunity following photodynamic therapy (65). Our group found that the blockage of TGF-β could convert N2 TANs to N1 TANs in murine models of mesothelioma and lung cancer (8).

Can human TANs exert antitumor (N1-like) activity? Although TANs isolated from early-stage lung cancers resemble murine antitumor N1 TANs, our data suggest that as tumors become larger, they become less stimulatory. It is thus possible that TANs from even more advanced tumors may become frankly protumorigenic. This concept, with regard to TANs, has recently been described in a murine tumor model. Mishalian et al. reported that TANs from early tumors were cytotoxic to tumor cells and produced higher levels of TNF-α, NO, and H_2O_2 compared with TANs in larger, established tumors (66). We are trying to test this "myeloid cell immunoediting" hypothesis with TANs from patients with advanced lung cancer (stages III and IV); however, this is logistically challenging since these individuals do not routinely undergo tumor resection and are managed with chemotherapy and radiation therapy.

Our study provides several explanations for the inconsistent data in the literature with regard to prognostic implications of TANs in cancer patients (11, 14–17). To date, most clinical studies have used immunohistochemical analyses of tumors to correlate the presence of granulocytes with prognosis. However, this approach is unable to assess the phenotype of these cells. In this study, we have demonstrated there is a heterogeneous expression of surface receptors on TANs. Thus, subpopulations of TANs likely exist in tumors at different stages of disease development and perform different functions. Also, since TANs might lose or change their antitumoral functions as the tumors progress, a simple neutrophil count in tumor tissue at any one time point (where the pro- versus antitumor status of the neutrophils is not known) may not be an accurate parameter for clinical prognosis.

In summary, our findings characterize tumor-infiltrating neutrophils in patients with lung cancer for the first time. Although the presence of a minor suppressive subpopulation of TANs cannot be excluded, our data suggest that TANs do not significantly contribute to inhibition of T cell responses in patients with early-stage lung cancer. Rather, the majority of neutrophils recruited into the tumor microenvironment undergo phenotypic and functional changes that result in the formation of cells that could potentially augment and support T cell responses. However, the in vitro conditions necessary for our experiments may not necessarily reflect what actually transpires in vivo. In addition, the ability of TANs to augment T cell responses is only one of many potential characteristics of antitumoral N1 neutrophils and does not entirely define TANs as antitumoral cells. In these studies, we were not able to assess the role of human TANs in the regulation of tumor cell proliferation, matrix remodeling, angiogenesis, and metastasis. Areas of future investigation in our laboratory are focused on deciphering subpopulations of neutrophils in human lung cancers and further characterization of the role of TANs in the regulation of tumor development using in vivo models. Ultimately, these findings may have important clinical implications, such as ways to take advantage of the T cell stimulatory activity of TANs and boost the efficacy of vaccines based on cytotoxic T lymphocyte induction.

Methods

Study design

A total of 86 patients with stage I–II lung cancer, who were scheduled for surgical resection, consented to the harvest of a portion of their tumor and blood for research purposes. All patients signed an informed consent document that was approved by the University of Pennsylvania Institutional Review Board, and met the following criteria: (a) histologically confirmed pulmonary squamous cell carcinoma (SCC) or adenocarcinoma (AC), (b) no prior chemotherapy or radiation therapy within 2 years, and (c) no other malignancy. Detailed characteristics of the patients can be found in Supplemental Table 1.

Reagents

The enzymatic cocktail for tumor digestion consisted of serum-free Hyclone Leibovitz L-15 medium supplemented with 1% penicillin-streptomycin, collagenase type I and IV (170 mg/l = 45–60 U/ml), collagenase type II (56 mg/l = 15–20 U/ml), DNase I (25 mg/l), and elastase (25 mg/l) (all from Worthington Biochemical). Cell culture reagents are described in Supplemental Methods.

Lymphocyte isolation from peripheral blood

Standard approaches were used. See Supplemental Methods.

Preparation of a single-cell suspension from lung tumor tissue

Surgically removed fresh lung tumors from patients were processed within 20 minutes of removal from the patient. In brief, the tumors were trimmed, sliced into small pieces, and digested for 1 hour at 37°C with shaking. After rbc lysis, cell viability was determined by trypan blue exclusion or Fixable Viability Dye eFluor 450 staining (Supplemental Figure 1B). If the viability of cells was less than 80%, dead cells were eliminated using a Dead Cell Removal Kit (Miltenyi Biotec Inc.). See Supplemental Methods for full details.

Tumor-conditioned medium

See Supplemental Methods.

Neutrophil isolation

Since temperature gradients can activate neutrophils, all tissues and reagents were maintained at a constant temperature during preparation. After tumor harvest, TANs and PBNs were prepared at room temperature and rapidly used.

TANs. A single-cell suspension was obtained by enzymatic digestion of tumor tissue. TANs were isolated from tumor cell suspensions using positive selection of $CD15^+$ or $CD66b^+$ cells with microbeads according to the manufacturer's instructions (Miltenyi Biotec Inc.). In some experiments, TANs were isolated by flow cytometric cell sorting based on the phenotype of TANs as $CD45^+CD11b^+CD66b^+CD15^+$. Sterile cell sorting was performed on the BD FACSAria II (BD Biosciences). For more details see Supplemental Methods.

PBNs. EDTA-anticoagulated peripheral blood was collected from lung cancer patients during surgery or from healthy donors, and density-gradient centrifugation was performed. To account for any possible effect of tissue digestion enzymes on neutrophil function, peripheral blood granulocytes were processed in a similar manner.

The purity and activation status of isolated TANs and PBNs were measured by flow cytometry for the granulocyte/myeloid markers CD66b, CD15, arginase-1 (Arg1), myeloperoxidase (MPO), and CD11b, and the activation markers CD62L and CD54. The TANs demonstrated high cell viability with minimal enzyme-induced premature cellular activation or cleavage of myeloid cell markers (Supplemental Figure 1). The purity of TANs and PBNs was typically higher than 94%. Isolates with less than 90% purity were discarded.

Flow cytometry

Flow cytometric analysis was performed according to standard protocols. Details about the Abs used are listed in Figure 3A. Matched-isotype Abs were used as controls. For more details see Supplemental Methods.

T cell proliferation assay

T cell proliferation induced by plate-bound anti–human CD3 (clone: OKT3) and/or anti-CD28 (clone: CD28.2) Abs was assessed using standard CFSE dilution methods. PBMCs or purified T cells (responders) were labeled with CFSE and cocultured in CD3/CD28–coated plates for 4 days in the complete cell culture medium. The CFSE signal was analyzed by flow cytometry on gated $CD4^+$ or $CD8^+$ lymphocytes. In several experiments, blocking Abs against CD86 (clone: IT2.2), CD80 (clone: 2D10), OX40L (clone: 11C3.1), 4-1BBL (clone: 5F4), CD54 (clone: HCD54), or CD40 (clone: 5C3) (all from Biolegend) were added to the cocultures of TANs and activated T cells at the concentration 1 μg/ml. In other experiments, the proliferation of T cells

was assessed by flow cytometry using the BrdU Flow Kit (BD Pharmingen). For more details see Supplemental Methods.

Allogeneic mixed lymphocyte reaction

Purified allogeneic T cells from healthy donor PBMCs were used as responders and reacted with irradiated, mature, monocyte-derived DCs (MoDCs) (inducers) from unrelated healthy donors. Immature MoDCs were prepared by culturing of adherent peripheral blood monocytes for 7 days in DMEM supplemented with 10% FBS, recombinant human GM-CSF (50 ng/ml), and IL-4 (50 ng/ml). To mature the MoDCs, LPS (100 ng/ml) was added to the cell culture for 24 hours before harvesting. The TANs or PBNs (regulators) were added to the DC-induced mixed lymphocyte reaction as "third-party cells" at a ratio of 1:0.25:1 (regulator/inducer/responder). Five days later, the proliferation of $CD4^+$ and $CD8^+$ T cells was measured using flow cytometric analysis of CFSE dilution.

Phagocytosis

The phagocytic activity of TANs and PBNs was assayed with the pHrodo Red *E. coli* BioParticles Phagocytosis Kit for flow cytometry (Life Technologies), according to the manufacturer's instructions.

Chemotaxis

We used a previously established protocol for fluorescence-based measurement of neutrophil migration in vitro across a polycarbonate filter (67) with minor modifications. See Supplemental Methods for details.

Neutrophil survival

Freshly isolated TANs or PBNs were cultured in complete cell culture medium in the presence or absence of 50% v/v of TCM for 20 hours. Neutrophil viability, apoptosis, and necrosis were measured using the FITC-Annexin V Apoptosis Detection Kit (Biolegend) and analyzed by flow cytometry, according to the manufacturer's instructions.

Measurement of ROS

The production of H_2O_2 in TANs and PBNs isolated from lung cancer patients and healthy donors was measured using Amplex Red Hydrogen Peroxide/Peroxidase Assay Kit (Invitrogen), according to the manufacturer's instructions. See Supplemental Methods for details.

Measurement of cytokines, chemokines, and growth factors

Single-cell suspensions were obtained from lung tumors by enzymatic digestion, as described above. TANs and PBNs were isolated from lung cancer patients, as described above. Both unseparated cells and isolated neutrophils from digested tumors, and PBNs, were resuspended in DME/F-12 1:1 medium with 10% FBS at a concentration of 1×10^6 cells/ml. Twenty-four hours later, cell culture supernatants were collected, filtered, and stored at –80°C until measurement. The levels of 30 cytokines/chemokines and growth factors were measured using the Cytokine Human Magnetic 30-Plex Panel for the Luminex platform (Invitrogen). The production of IFN-γ, IL-10, and GM-CSF was measured with commercial ELISA kits purchased from BD Bioscience.

Immunohistochemistry

The tumor microarrays (TMAs) were constructed from formalin-fixed, paraffin-embedded tumor and adjacent normal specimens collected at the time of surgical resection. Sections from 45 AC and 25 SCC patients were analyzed. After standard antigen retrieval, the TMAs were double-

stained with an anti-cytokeratin Ab to label cancer cells and an Ab against human MPO to label neutrophils. Slide imaging was performed on a Vectra automated imaging robot and analyzed using Inform analysis software. Data are expressed as the intraepithelial or stromal hematopoietic cell density per square millimeter of tumor tissue. In addition, we costained for neutrophils (MPO), APCs (HLA-DR), and T cells (CD3), using their respective Abs. See Supplemental Methods for details.

Statistics

All data were tested for normal distribution of variables. Comparisons between 2 groups were assessed with a 2-tailed Student's *t* test for paired and unpaired data if data were normally distributed. Nonparametric Wilcoxon matched-pairs test and Mann-Whitney unpaired test were used when the populations were not normally distributed. Likewise, multiple groups were analyzed by 1-way ANOVA with corresponding Tukey's multiple comparison test if normally distributed, or the Kruskal-Wallis with Dunn's multiple comparison test if not. Nonparametric Spearman test was used for correlation analysis. All statistical analyses were performed with GraphPad Prism 6. A *P* value less than 0.05 was considered statistically significant.

Study approval

The study was approved by the University of Pennsylvania Institutional Review Board (IRB no. 813004). All patients signed an informed consent document.

Address correspondence to: Evgeniy Eruslanov, Division of Thoracic Surgery, Department of Surgery, Perelman School of Medicine at the University of Pennsylvania, 3400 Spruce Street, 6 White, Philadelphia, Pennsylvania 19104, USA. Phone: 610.772.5624; E-mail: Evgeniy.Eruslanov@uphs.upenn.edu.

1. Balkwill F, Charles KA, Mantovani A. Smoldering and polarized inflammation in the initiation and promotion of malignant disease. *Cancer Cell.* 2005;7(3):211–217.
2. Sica A, et al. Origin and functions of tumor-associated myeloid cells (TAMCs). *Cancer Microenviron.* 2012;5(2):133–149.
3. Heusinkveld M, van der Burg SH. Identification and manipulation of tumor associated macrophages in human cancers. *J Transl Med.* 2011;9:216.
4. Galdiero MR, Garlanda C, Jaillon S, Marone G, Mantovani A. Tumor associated macrophages neutrophils in tumor progression. *J Cell Physiol.* 2013;228(7):1404–1412.
5. Brandau S, Dumitru CA, Lang S. Protumor and antitumor functions of neutrophil granulocytes. *Semin Immunopathol.* 2013;35(2):163–176.
6. Houghton AM. The paradox of tumor-associated neutrophils: Fueling tumor growth with cytotoxic substances. *Cell Cycle.* 2010;9(9):1732–1737.
7. Piccard H, Muschel RJ, Opdenakker G. On the dual roles and polarized phenotypes of neutrophils in tumor development and progression. *Crit Rev Oncol Hematol.* 2012;82(3):296–309.
8. Fridlender ZG, et al. Polarization of tumor-associated neutrophil phenotype by TGF-β: "N1" versus "N2" TAN. *Cancer Cell.* 2009;16(3):183–194.
9. Mestas J, Hughes CC. Of mice and not men: differences between mouse and human immunology. *J Immunol.* 2004;172(5):2731–2738.
10. Seok J, et al. Genomic responses in mouse models poorly mimic human inflammatory diseases. *Proc Natl Acad Sci U S A.* 2013;110(9):3507–3512.
11. Trellakis S, et al. Polymorphonuclear granulocytes in human head and neck cancer: enhanced inflammatory activity, modulation by cancer cells and expansion in advanced disease. *Int J Cancer.* 2011;129(9):2183–2193.
12. Jensen HK, Donskov F, Marcussen N, Nordsmark M, Lundbeck F, von der Maase H. Presence of intratumoral neutrophils is an independent prognostic factor in localized renal cell carcinoma. *J Clin Oncol.* 2009;27(28):4709–4717.
13. Jensen TO, et al. Intratumoral neutrophils and plasmacytoid dendritic cells indicate poor prognosis and are associated with pSTAT3 expression in AJCC stage I/II melanoma. *Cancer.* 2012;118(9):2476–2485.
14. Li YW, et al. Intratumoral neutrophils: A poor prognostic factor for hepatocellular carcinoma following resection. *J Hepatol.* 2011;54(3):497–505.
15. Rao HL, et al. Increased intratumoral neutrophil in colorectal carcinomas correlates closely with malignant phenotype and predicts patients' adverse prognosis. *PLoS One.* 2012;7(1):e30806.
16. Caruso RA, Bellocco R, Pagano M, Bertoli G, Rigoli L, Inferrera C. Prognostic value of intratumoral neutrophils in advanced gastric carcinoma in a high-risk area in northern italy. *Mod Pathol.* 2002;15(8):831–837.
17. Carus A, Ladekarl M, Hager H, Pilegaard H, Nielsen PS, Donskov F. Tumor-associated neutrophils and macrophages in non-small cell lung cancer: No immediate impact on patient outcome. *Lung Cancer.* 2013;81(1):130–137.
18. Ilie M, et al. Predictive clinical outcome of the intratumoral CD66b-positive neutrophil-to-CD8-positive T-cell ratio in patients with resectable nonsmall cell lung cancer. *Cancer.* 2012;118(6):1726–1737.
19. Radsak M, Iking-Konert C, Stegmaier S, Andrassy K, Hansch GM. Polymorphonuclear neutrophils as accessory cells for T-cell activation: major histocompatibility complex class II restricted antigen-dependent induction of T-cell proliferation. *Immunology.* 2000;101(4):521–530.
20. Ashtekar AR, Saha B. Poly's plea: membership to the club of APCs. *Trends Immunol.* 2003;24(9):485–490.
21. Potter NS, Harding CV. Neutrophils process exogenous bacteria via an alternate class I MHC processing pathway for presentation of peptides to T lymphocytes. *J Immunol.* 2001;167(5):2538–2546.
22. Reali E, et al. Polymorphonuclear neutrophils pulsed with synthetic peptides efficiently activate memory cytotoxic T lymphocytes. *J Leukoc Biol.* 1996;60(2):207–213.
23. Pillay J, et al. A subset of neutrophils in human systemic inflammation inhibits T cell responses through mac-1. *J Clin Invest.* 2012;122(1):327–336.
24. Schmielau J, Finn OJ. Activated granulocytes and granulocyte-derived hydrogen peroxide are the underlying mechanism of suppression of t-cell function in advanced cancer patients. *Cancer Res.* 2001;61(12):4756–4760.
25. Munder M, et al. Suppression of T-cell functions by human granulocyte arginase. *Blood.* 2006;108(5):1627–1634.
26. Gorgun GT, et al. Tumor-promoting immune-suppressive myeloid-derived suppressor cells in the multiple myeloma microenvironment in humans. *Blood.* 2013;121(15):2975–2987.
27. Gabrilovich DI, Nagaraj S. Myeloid-derived suppressor cells as regulators of the immune system. *Nat Rev Immunol.* 2009;9(3):162–174.
28. Eruslanov E, et al. Circulating and tumor-infiltrating myeloid cell subsets in patients with bladder cancer. *Int J Cancer.* 2012;130(5):1109–1119.
29. Pignatti P, et al. Downmodulation of CXCL8/IL-8 receptors on neutrophils after recruitment in the airways. *J Allergy Clin Immunol.* 2005;115(1):88–94.
30. Fortunati E, Kazemier KM, Grutters JC, Koenderman L, Van den Bosch VJMM. Human neutrophils switch to an activated phenotype after homing to the lung irrespective of inflammatory disease. *Clin Exp Immunol.* 2009;155(3):559–566.
31. Liu CY, et al. Population alterations of L-arginase- and inducible nitric oxide synthase-expressed CD11b+/CD14(–)/CD15+/CD33+ myeloid-derived suppressor cells and CD8+ T lymphocytes in patients with advanced-stage non-small cell lung cancer. *J Cancer Res Clin Oncol.* 2010;136(1):35–45.
32. Gabrilovich DI, Ostrand-Rosenberg S, Bronte V. Coordinated regulation of myeloid cells by tumours. *Nat Rev Immunol.* 2012;12(4):253–268.

33. Hartl D, et al. Infiltrated neutrophils acquire novel chemokine receptor expression and chemokine responsiveness in chronic inflammatory lung diseases. *J Immunol*. 2008;181(11):8053–8067.

34. de Kleijn S, et al. IFN-γ-stimulated neutrophils suppress lymphocyte proliferation through expression of PD-L1. *PLoS One*. 2013;8(8):e72249.

35. Zhu C, et al. The tim-3 ligand galectin-9 negatively regulates T helper type 1 immunity. *Nat Immunol*. 2005;6(12):1245–1252.

36. van Vliet SJ, Gringhuis SI, Geijtenbeek TB, van Kooyk Y. Regulation of effector T cells by antigen-presenting cells via interaction of the C-type lectin MGL with CD45. *Nat Immunol*. 2006;7(11):1200–1208.

37. Rygiel TP, Meyaard L. CD200R signaling in tumor tolerance and inflammation: A tricky balance. *Curr Opin Immunol*. 2012;24(2):233–238.

38. Zhou L, et al. Impact of human granulocyte and monocyte isolation procedures on functional studies. *Clin Vaccine Immunol*. 2012;19(7):1065–1074.

39. Gao JL, et al. Impaired host defense, hematopoiesis, granulomatous inflammation and type 1-type 2 cytokine balance in mice lacking CC chemokine receptor 1. *J Exp Med*. 1997;185(11):1959–1968.

40. Youn JI, Collazo M, Shalova IN, Biswas SK, Gabrilovich DI. Characterization of the nature of granulocytic myeloid-derived suppressor cells in tumor-bearing mice. *J Leukoc Biol*. 2012;91(1):167–181.

41. Thewissen M, Damoiseaux J, van de Gaar J, Tervaert JW. Neutrophils and T cells: Bidirectional effects and functional interferences. *Mol Immunol*. 2011;48(15–16):2094–2101.

42. Fontenot JD, Gavin MA, Rudensky AY. Foxp3 programs the development and function of CD4+CD25+ regulatory T cells. *Nat Immunol*. 2003;4(4):330–336.

43. Kobayashi SD, Voyich JM, Whitney AR, DeLeo FR. Spontaneous neutrophil apoptosis and regulation of cell survival by granulocyte macrophage-colony stimulating factor. *J Leukoc Biol*. 2005;78(6):1408–1418.

44. Yoshimura T, Takahashi M. IFN-γ-mediated survival enables human neutrophils to produce MCP-1/CCL2 in response to activation by TLR ligands. *J Immunol*. 2007;179(3):1942–1949.

45. Lentzsch S, Gries M, Janz M, Bargou R, Dorken B, Mapara MY. Macrophage inflammatory protein 1-alpha (MIP-1α) triggers migration and signaling cascades mediating survival and proliferation in multiple myeloma (MM) cells. *Blood*. 2003;101(9):3568–3573.

46. Doedens AL, et al. Macrophage expression of hypoxia-inducible factor-1 α suppresses T-cell function and promotes tumor progression. *Cancer Res*. 2010;70(19):7465–7475.

47. Marigo I, et al. Tumor-induced tolerance and immune suppression depend on the C/EBPβ transcription factor. *Immunity*. 2010;32(6):790–802.

48. Corzo CA, et al. HIF-1α regulates function and differentiation of myeloid-derived suppressor cells in the tumor microenvironment. *J Exp Med*. 2010;207(11):2439–2453.

49. Kusmartsev S, Nefedova Y, Yoder D, Gabrilovich DI. Antigen-specific inhibition of CD8+ T cell response by immature myeloid cells in cancer is mediated by reactive oxygen species. *J Immunol*. 2004;172(2):989–999.

50. Biswas SK, Mantovani A. Macrophage plasticity and interaction with lymphocyte subsets: cancer as a paradigm. *Nat Immunol*. 2010;11(10):889–896.

51. Fridlender ZG, et al. Using macrophage activation to augment immunotherapy of established tumours. *Br J Cancer*. 2013;108(6):1288–1297.

52. Guiducci C, Vicari AP, Sangaletti S, Trinchieri G, Colombo MP. Redirecting in vivo elicited tumor infiltrating macrophages and dendritic cells towards tumor rejection. *Cancer Res*. 2005;65(8):3437–3446.

53. Nozawa H, Chiu C, Hanahan D. Infiltrating neutrophils mediate the initial angiogenic switch in a mouse model of multistage carcinogenesis. *Proc Natl Acad Sci U S A*. 2006;103(33):12493–12498.

54. Jablonska J, Leschner S, Westphal K, Lienenklaus S, Weiss S. Neutrophils responsive to endogenous IFN-β regulate tumor angiogenesis and growth in a mouse tumor model. *J Clin Invest*. 2010;120(4):1151–1164.

55. Spicer JD, et al. Neutrophils promote liver metastasis via mac-1-mediated interactions with circulating tumor cells. *Cancer Res*. 2012;72(16):3919–3927.

56. Sandilands GP, McCrae J, Hill K, Perry M, Baxter D. Major histocompatibility complex class II (DR) antigen and costimulatory molecules on in vitro and in vivo activated human polymorphonuclear neutrophils. *Immunology*. 2006;119(4):562–571.

57. Watts TH. TNF/TNFR family members in costimulation of T cell responses. *Annu Rev Immunol*. 2005;23:23–68.

58. Shao Z, Schwarz H. CD137 ligand, a member of the tumor necrosis factor family, regulates immune responses via reverse signal transduction. *J Leukoc Biol*. 2011;89(1):21–29.

59. Chacon JA, et al. Co-stimulation through 4-1BB/CD137 improves the expansion and function of CD8(+) melanoma tumor-infiltrating lymphocytes for adoptive T-cell therapy. *PLoS One*. 2013;8(4):e60031.

60. Hernandez-Chacon JA, et al. Costimulation through the CD137/4-1BB pathway protects human melanoma tumor-infiltrating lymphocytes from activation-induced cell death and enhances antitumor effector function. *J Immunother*. 2011;34(3):236–250.

61. Musiani P, et al. Role of neutrophils and lymphocytes in inhibition of a mouse mammary adenocarcinoma engineered to release IL-2, IL-4, IL-7, IL-10, IFN-α, IFN-γ, and TNF-α. *Lab Invest*. 1996;74(1):146–157.

62. Giovarelli M, et al. Tumor rejection and immune memory elicited by locally released LEC chemokine are associated with an impressive recruitment of APCs, lymphocytes, and granulocytes. *J Immunol*. 2000;164(6):3200–3206.

63. Colombo MP, et al. Granulocyte colony-stimulating factor gene transfer suppresses tumorigenicity of a murine adenocarcinoma in vivo. *J Exp Med*. 1991;173(4):889–897.

64. Suttmann H, et al. Neutrophil granulocytes are required for effective bacillus calmette-guerin immunotherapy of bladder cancer and orchestrate local immune responses. *Cancer Res*. 2006;66(16):8250–8257.

65. Kousis PC, Henderson BW, Maier PG, Gollnick SO. Photodynamic therapy enhancement of antitumor immunity is regulated by neutrophils. *Cancer Res*. 2007;67(21):10501–10510.

66. Mishalian I, Bayuh R, Levy L, Zolotarov L, Michaeli J, Fridlender ZG. Tumor-associated neutrophils (TAN) develop pro-tumorigenic properties during tumor progression. *Cancer Immunol Immunother*. 2013;62(11):1745–1756.

67. Frevert CW, Wong VA, Goodman RB, Goodwin R, Martin TR. Rapid fluorescence-based measurement of neutrophil migration in vitro. *J Immunol Methods*. 1998;213(1):41–52.